Z. Phys. Chem. / **DOI** 10.1524/zpch.2013.0405


# 7D Quantum Dynamics of $H_2$ Scattering from Cu(111): The Accuracy of the Phonon Sudden Approximation

By Matteo Bonfanti[1], Mark F. Somers[1], Cristina Díaz[2], Heriberto Fabio Busnengo[3], and Geert-Jan Kroes[1,*]

[1] Leiden Institute of Chemistry, Universiteit Leiden, Gorlaeus Laboratories, Einsteinweg 55, 2333 CC, Leiden, Netherlands
[2] Departamento de Química, Universidad Autónoma de Madrid, Cantoblanco, 28049 Madrid, Spain
[3] Instituto de Física Rosario (CONICET-UNR) and Facultad de Ciencias Exactas, Ingeniería y Agrimensura, Universidad Nacional de Rosario, Av. Pellegrini 250, 2000 Rosario, Argentina

(Received February 25, 2013; accepted in revised form April 18, 2013)
(Published online June 17, 2013)

***Molecule-Surface Scattering / Hydrogen Dissociative Chemisorption / Scattering Quantum Dynamics / Phonon Sudden Approximation / Potential Energy Surface / Density Functional Theory***

The correct prediction of elementary processes occurring when $H_2$ scatters from a metal surface is one of the main challenges of surface science. In the field, the scattering of $H_2$ from Cu(111) has been considered a prototype system for activated dissociative chemisorption. Experimental and theoretical work suggested that a proper description of some scattering experiments on this system might require going beyond the static surface approximation, to consider how the motion of the Cu atoms affects the scattering event. Previous work suggested that important effects of phonons on the dynamics can be incorporated in the Potential Energy Surface (PES) by including four degrees of freedom, that have approximately additive couplings with the hydrogen molecule: the 3 dimensional motion of the nearest 1$^{st}$ layer copper atom and the displacement of the nearest 2$^{nd}$ layer copper atom along the direction perpendicular to the surface [3]. In the present work, we extend the 6D dynamical model by including the perpendicular motion of the 2$^{nd}$ layer surface atom and we study this novel dynamical model with two techniques: an approximate method based on the Phonon Sudden Approximation (PSA) and an exact description using 7D wavepacket quantum dynamics. We consider how the inclusion and the excitation of the lattice degree of freedom affect some relevant processes: dissociative chemisorption, vibrational excitation of $H_2$ and state-to-state scattering probabilities fully resolved with respect to the vibrational states of the surface. We show that the PSA works in an excellent way for the system, thereby suggesting that this might be a viable way to study higher dimensional quantum models, incorporating four surface degrees of freedom that appear to be most relevant for $H_2$ scattering.

* Corresponding author. E-mail: g.j.kroes@chem.leidenuniv.nl

## 1. Introduction

Potential Energy Surfaces (PESs) have been extremely useful in the understanding of elementary processes at surfaces. Starting from gas-phase problems [49], PESs were soon used also for the study of reactions of molecules at metal surfaces, as shown by the 1932 seminal work of Lennard-Jones on adsorption and diffusion on solid surfaces [35]. For these systems, many experimental trends have been rationalized and understood on the basis of PESs. In some cases quantitative agreement with experiments was obtained, even if in most of the theoretical studies the surface was assumed to be static and its electronic degrees of freedom were neglected. On the other end, substantial electron-hole pair excitation was observed in scattering experiments with metals surfaces showing a deep chemisorption well [21]. In the case of vibrationally excited NO scattering from a metal with a low work function, electron emission was even detected [61]. Furthermore, there is evidence that surface phonons in some cases highly affect the dissociative chemisorption probability, particularly when the molecule is heavier than $H_2$ [36,42] or when its incidence energy is below the classical threshold to reaction [40].

With respect to diatom scattering from metal surfaces, $H_2$ on Cu(111) has become an invaluable benchmark problem. Indeed, for this system a wide range of detailed experiments investigating the influence of translational, rotational and vibrational energy on both dissociative chemisorption and scattering is available [2,24,30–32,37,38,40,50–52].

From a theoretical point of view, much progress has been made over the last twenty years. At the beginning, theoretical studies were performed with a limited number of $H_2$ degrees of freedom with the aim of clarifying the mechanisms underlying reactive scattering [10–15,22,58]. Next, quantum dynamics calculations based on DFT potential energy surfaces including all degrees of freedom of $H_2$ [7,28,47] became feasible and were used for a qualitative and quantitative comparison with experiments [7,9,16–18,34,44,59]. More recently, chemical accuracy was achieved by Díaz *et al.* [16,18] by means of the Specific Reaction Parameter (SRP) approach to Density Functional Theory (DFT) [6]. In the SRP-DFT method implemented by the authors, the exchange-correlation functional was computed as a weighted average of suitable Generalized Gradient Approximation (GGA) functionals. Adjusting the mixing coefficient to reproduce a specific $D_2$/Cu(111) molecular beam sticking experiment as a function of incidence energy [50], a reliable 6D PES was obtained.

Like most of the dynamical simulations of $H_2$-metal surface scattering thus far, this latter work assumed a perfect crystal static surface and no electron-hole pair excitations. Although these approximations proved to yield accurate results for most observables, for two particular experiments they might not be adequate. Firstly, the associative desorption experiments that were used to measure the rotational quadrupole alignment parameter [32] were performed at high surface temperature ($T_S = 925$ K). Secondly, the comparison between calculations and experiments on vibrational excitation of $H_2$ scattering from Cu(111) [51] suggests that an accurate description of this process requires the inclusion of surface motion [34].

This suggests that for a completely correct description of the available experiments of $H_2$/Cu(111) the inclusion of the lattice motion may be necessary. This challeng-

ing goal is being currently pursued with different methodologies. By means of *Ab Initio* Molecular Dynamics (AIMD), Nattino *et al.* proved that the inclusion of surface temperature effects allows a better prediction of the rotational quadrupole alignment parameter [41]. Furthermore, Wijzenbroek and Somers pointed out the importance of the temperature of the lattice even at a level at which energy transfer to surface phonons is not allowed, *via* a simplified molecular dynamics study on the system [62]. Finally, Sahoo *et al.* addressed the problem with an effective hamiltonian derived from a mean-field approximation to the phonon modes and showed the importance of the surface modes directed along the $Z$-axis [55,56].

In our previous work we have analyzed the coupling of the $H_2$ to the metal surface phonons at a SRP-DFT level [3]. To this aim, we have adopted a theoretical picture first introduced by Nave and Jackson [43] in relation to the scattering of $CH_4$/Ni and $CH_4$/Pt. We have shown that as long as the perpendicular motion of the lattice atoms is taken into account, we can distinguish the effect of first and second layer atoms motion from the way they affect the Transition States (TS) of $H_2$ dissociation. The motion along $Z$ of the first layer atoms leads mostly to a mechanical coupling, *i. e.* the geometry of the transition state changes almost without an increase or decrease of the barrier height. On the contrary, $Z$ motion of the second layer atoms leads to an electronic coupling: the transition state geometry is mostly unaffected while the barrier height changes.

Our previous work also suggests that important effects of surface phonons can be incorporated by including four degrees of freedom in the dynamical model: the three-dimensional motion of the nearest first layer copper atom and the one-dimensional motion of the second layer atom in the direction perpendicular to the surface. The dependence on these four degrees of freedom can easily be incorporated in the PES, since the effects are small and, to a good approximation, additive, and a parabolic dependence on the four coordinates suffices. The problem that we address here is how to incorporate the four additional coordinates in a quantum dynamical treatment. We use a 7D model including the perpendicular motion of the second layer atom as a testing ground for an approximate approach based on the vibrational sudden approximation [4]. The key idea of this approximation, earlier introduced in quantum scattering of $H_2$ from Pd(100) by Olsen *et al.* [45] and recently applied by Tiwari *et al.* in the case of $CH_4$/Ni [60], is to compute the scattering probability as an average of the probabilities computed by fixing the lattice atom in different positions. We prefer this methodology over a mean field approach [55,56] because we can in this way exploit the fact that surface atom motion is slow relative to molecular motion. We will show in the following that our sudden approach is successful and opens the way for the study of higher dimensional dynamical models.

The goal of the present paper is then twofold. First, we present a novel 7D description of the system including only the motion of a second layer atom perpendicular to the surface (which in the following will be addressed as our "dynamical model") and determine whether this extra degree of freedom is relevant for the correct description of surface temperature effects. Second, we assess the accuracy of a sudden approach in the description of the effects which are due to our particular surface atom motion.

This paper is subdivided as follows. In Sect. 2 we present the dynamical model adopted in the present work, in light of the findings of [3]. In Sect. 3 we describe the theoretical methods used for the development of the PES and for the dynamical simu-

lations. The results are shown and discussed in Sect. 4. Finally, some conclusions are presented in Sect. 5.

## 2. The dynamical model

The model we adopted in this study extends the previous work by Díaz *et al.* by including one additional coordinate describing one of the relevant surface degrees of freedom of the copper lattice. The choice of this additional coordinate has been made based on the theoretical evidence available for the system. In our previous DFT study [3] we showed that the reaction path for $H_2$ dissociation is predominantly affected by the full three-dimensional motion of the first layer atoms and the one-dimensional perpendicular motion of the second layer atoms.

Since the model approach of Sahoo *et al.* [55] suggested that the perpendicular motion is the most dynamically effective and since Debye-Waller attenuation of diffractive scattering can be described purely on the basis of surface atom motion perpendicular to the surface, we are most interested in the perpendicular displacements. We can then focus here on only two degrees of freedom: one for the first layer atoms and one for the second layer atoms.

In [3] we showed that these two displacements have approximately additive effects. Besides, following the same distinction between mechanical and electronic coupling discussed in [43], these two motions have a very distinctive behaviour. While the first layer motion has mainly a mechanical effect, the second layer motion has mainly an electronic effect.

Figure 1 shows how the motion of a second layer Cu atom affects a set of relevant transition states, obtained by fixing the impact site and the orientation of the $H_2$ molecule on the (111) surface (for the meaning of the acronyms of transition state geometries, see Fig. 2, lower panel). For each of these TS, the graph reports the dependence on $Q$, *i. e.* the copper displacement, of the $Z$ value of the reaction barrier geometry (top panel) and of the barrier height (lower panel). The curves for the dependence on the $Z$ coordinate of the t2h(120°) and TtH transitions states are not reported since a negligible change (as apparent from very small values of $\alpha$) was found.

For small displacements of the Cu atoms, both effects are roughly linear in the surface coordinate. Following [43], we define two linear parameters $\alpha$ and $\beta$ by

$$\Delta Z_b = \alpha Q$$
$$\Delta E_b = -\beta Q$$

The parameter $\alpha$ hence accounts for the barrier displacement in the $Z$ direction. The parameter $\beta$, on the other hand, describes the change in barrier height due to the motion of the lattice atom.

If we displace a 2$^{nd}$ layer Cu atom, the dissociation geometry does not undergo large changes: within a few hundredths of Å, we can therefore assume that the dissociation barrier geometries are not dependent on $Q$. In contrast, relevant changes are found in the barrier height. For $Q = -0.2$ Å, the BtH, t2h(120°) and hcp(0°) barrier heights are lowered by 48 meV, 42 meV, 65 meV respectively.

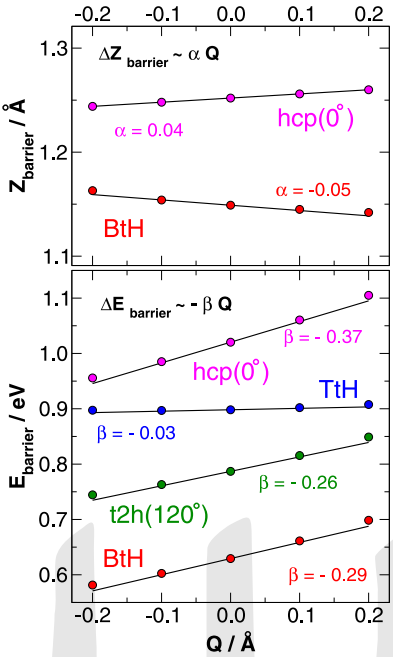


**Fig. 1.** $H_2$ center of mass $Z$ coordinate (top panel) and barrier heights (lower panel) of some representative dissociation geometries as a function of the lattice coordinate $Q$, the displacement of the second layer atom perpendicular to the surface. The points computed by DFT have been fitted with a linear model, and the fitting parameters $\alpha$ (dimensionless) and $\beta$ (in eV Å$^{-1}$) are reported in the graph (see the text for the meaning of $\alpha$ and $\beta$).

This effect can be understood in terms of the d-band model of $H_2$-surface reactivity [26]. Near the impact site, the motion of the 2$^{nd}$ layer atom towards the bulk has analogous effects as an expansion of the lattice. The smaller overlap between the orbitals of the substrate atoms reduces the width of the d-band, causing an upshift of the band if it is more than half-filled [57]. This leads to a lower barrier height for dissociative adsorption [57].

The same analysis performed by considering the perpendicular displacement of a first layer copper atom showed that this kind of motion affects mostly the TS geometry and hardly changes the barrier height. This kind of effect has been already studied from the dynamical point of view *via* the Surface Oscillator (SO) model [29], also in the case of the $H_2$/Cu(111) system [16]. In contrast, the effect of the electronic coupling on $H_2$-system scattering has been studied so far only in low dimensional model systems [19]. In the light of this, we decided to start extending the scattering model with the inclusion of the 2$^{nd}$ layer atom.

In conclusion, we decided to investigate a 7D dynamical model including all the 6 degrees of freedom of the $H_2$ molecule and an additional 7$^{th}$ degree of freedom to describe the displacement of the second layer atom nearest to $H_2$, in the direction perpendicular to the surface. The coordinate system that we adopted is depicted in Fig. 3 and contains the center of mass of the $H_2$ molecule – $X$, $Y$ and $Z$ – the polar coordinate of the H-H bond – $r$, $\vartheta$ and $\varphi$ – and the motion of the copper atom $Q$.

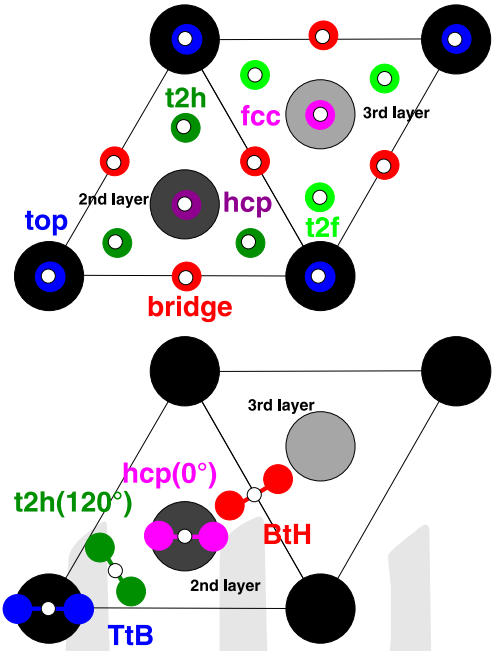


**Fig. 2.** Top panel: the high symmetry sites of the (111) surface: top (in blue), bridge (in red), hcp (hollow, above a 2nd layer Cu, in dark magenta), fcc (hollow, above a 3rd layer Cu, in light magenta), t2h (halfway between top and hcp, in dark green) or t2f (halfway between top and fcc, in light green). Lower panel: the reference barrier geometries considered: TtB (top to bridge, in blue), t2h(120°) (t2h site, with $\varphi = 120°$, in green), hcp(0°) (hcp site, with $\varphi = 0°$, in magenta) and BtH (bridge to hollow, in red).

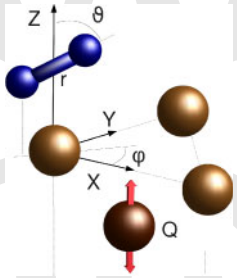


**Fig. 3.** The 7D dynamical model adopted in the present work, including 6 degrees of freedom for the $H_2$ molecule and a single coordinate for a second layer lattice copper atom.

# 3. Methods

## 3.1 Potential energy surface

To describe the interaction between the hydrogen molecule and the surface, we computed more than 18 000 points with DFT. To rely on a accurate description of the energetics of the $H_2$/Cu(111) system, we followed the SRP approach to DFT, as im-

plemented by Díaz *et al.* in [16,18]. In particular, these calculations were carried out with DACAPO [1]. The exchange-correlation energy was computed as a weighted average of two GGA functionals: the Revised Perdew-Burke-Ernzerhof (RPBE) functional [27] and the Perdew-Wang 1991 (PW91) functional [46]. The mixing parameter value ($x = 0.43$) was chosen by Díaz to reproduce the reaction probabilities measured in $D_2 + Cu(111)$ molecular beam experiments [38,50].

As in [16–18], the Cu surface is described with a supercell using four layers of metal atoms, employing a $2 \times 2$ hexagonal surface unit cell. A vacuum space of 13.0 Å is placed between the four-layer slabs to avoid artifacts due to the use of periodic boundary conditions in the direction perpendicular to the slab. The first Brillouin zone is sampled with a $8 \times 8 \times 1$ Monkhorst-Pack grid of **k**-points. A plane wave basis set with an energy cutoff of 350 eV is used in the calculations.

To represent the DFT points with an analytical function, we first developed three different 6D potential energy surfaces including all the coordinates of the $H_2$ molecule for a given $Q$ displacement. The values $Q = -0.2$ Å, 0.0 Å, 0.2 Å were chosen, on the basis of the vibrational frequency of the 2$^{nd}$ layer atom displacement reported in [3]. Each 6D PES for a fixed $Q$ was fitted with the Corrugation Reducing Procedure (CRP) methodology [5]. Next the dependence on the 7$^{th}$ degree of freedom was introduced by interpolating a parabolic function in $Q$ along these 3 6D PESs. Our previous results have shown that for small oscillations of the copper atom this is a good approximation of the $Q$ dependence for both the strain and the coupling potential [3].

### 3.2 Quantum wavepacket dynamics and vibrational sudden approximation

We performed state-resolved quantum dynamical simulation of the scattering event by means of time-dependent wavepacket calculations. The wavefunction was represented by a Discrete Variable Representation (DVR), on a grid chosen in accordance with the properties of each coordinate. In particular, the additional 7$^{th}$ degree of freedom was described with a Hermite-Gauss DVR using the harmonic frequency of the bare surface $Q$ oscillation. The initial state was built to describe a definite ($v$, $J$, $M_J$) rovibrational state of the molecule, colliding at normal incidence with the surface in a given phonon vibrational state $n$. Here, $v$ is the vibrational quantum number of the molecule, $J$ is the rotational quantum number and $M_J$ the projection of $J$ on the surface normal. The motion along $Z$ is initially represented by a gaussian wavepacket with a momentum directed towards the surface.

We performed the time-evolution of the wavefunction according to the Schrödinger equation within the Split Operator scheme. The reflected wave packet was analyzed using a scattering amplitude formalism [39], namely by fourier transforming the asymptotic projection of the the wavepacket on the scattering eigenstates. Further details on the methodology are reported in [16,48], while a detailed list of the relevant parameters adopted for the calculations can be found in Table 1.

In addition to full 7D quantum calculations, we also implemented and tested the Phonon Sudden Approximation (PSA). The vibrational sudden approximation is a methodology introduced in gas-phase scattering by Bowman *et al.* [4] and first applied to phonons in a surface reactive scattering problem by Olsen *et al.* [45]. In this approximate description, the scattering amplitude for the 7D dynamical event is expressed as an

**Table 1.** Parameters of the 7D quantum dynamics calculations of $H_2$ scattering from Cu(111) (data in atomic units).

| | |
|---|---|
| Nr. of points in $Z$ | 120 |
| Minumum value of $Z$ | −1.00 |
| Grid spacing in $Z$ | 0.12 |
| Nr. of points in $r$ | 56 |
| Minumum value of $r$ | 0.40 |
| Grid spacing in $r$ | 0.15 |
| Nr. of points in $X/Y$ | 18 |
| Maximum $J$ in the basis set | 16/17 |
| Nr. of points in $Q$ | 16 |
| Total propagation time | 30000 |
| Time step | 5 |
| Initial average $Z$ of the wavepacket | 12.00 |
| Initial parallel momentum along $X/Y$ | 0.0 |
| $Z$ of the analysis plane | 9.08 |

average over the vibrational degree of freedom $Q$ of 6D scattering amplitudes. In turn, these 6D calculations are scattering simulations in which the copper atom is frozen in different positions around equilibrium. In the following we will denote full quantum dynamical calculations by "7D" and calculations using the phonon sudden approximation by "6 + 1D".

Let $S^{\text{sudden}}(\mathbf{f} \leftarrow \mathbf{i};\, Q)$ be the 6D scattering amplitude computed for a molecule going from initial state $\mathbf{i}$ to final state $\mathbf{f}$, fixing the position of the surface degree position at the $Q$ value. Labelling the initial and final vibrational state of the surface with $n$ and $n'$, the 7D scattering matrix in the phonon sudden approximation is given by

$$S(\mathbf{f}\ n' \leftarrow \mathbf{i}\, n) = \int dQ\, \chi^{\star}_{n'}(Q)\, S^{\text{sudden}}(\mathbf{f} \leftarrow \mathbf{i};\, Q)\, \chi_n(Q)$$

where $\chi_n(Q)$ and $\chi_{n'}(Q)$ are two eigenfunctions of the vibrational hamiltonian of the surface.

When modeling experiments in which only the $H_2$ final state is relevant, we are not interesented in resolving the results over the final state of the surface degree of freedom. We can then obtain the molecular state-to-state scattering probability by summing over the final phonon state of the surface:

$$P_{\text{scatter}}(\mathbf{f} \leftarrow \mathbf{i}\, n) = \sum_{n'} \left| S(\mathbf{f}\ n' \leftarrow \mathbf{i}\, n) \right|^2$$

Substituting the phonon approximation expression and using the completeness of the states $\chi_{n'}$, the molecular state-to-state reaction probability is given by the average of the scattering probability, with a weight which is given by the square of the initial vibrational eigenfunction

$$P_{\text{scatter}}(\mathbf{f} \leftarrow \mathbf{i}\, n) = \int dQ \left| S^{\text{sudden}}(\mathbf{f} \leftarrow \mathbf{i};\, Q) \right|^2 |\chi_n(Q)|^2$$

In conclusion, in the phonon sudden approximation the molecular state-to-state scattering probability depends only on the absolute value of the scattering amplitude,

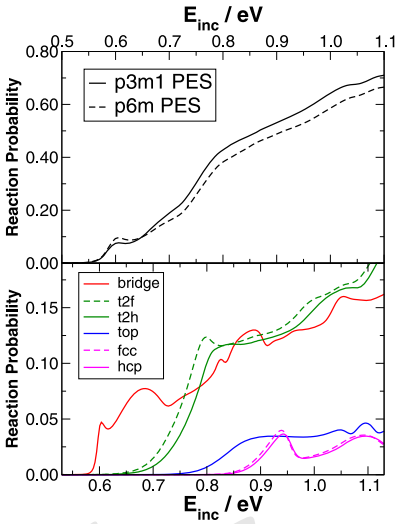


**Fig. 4.** Comparison between p3m1 and p6m potentials. In the top panel, the 6D reaction probability computed within the static surface model for the p3m1 PES (solid line) and the p6m PES (dashed line) is shown. In the lower panel, the 4D reaction probability are shown for the calculations with the $X, Y$ components of the $H_2$ center of mass fixed at one the high symmetry sites of the surface and the phonon coordinate frozen at $Q = 0$.

and not on its phase. The phase affects the scattering probability only if the full dependence of the scattering probability on the final phonon state is retained.

From a physical point of view the sudden approximation accounts for *quasi*-static effects, that are expected for weakly coupled degrees of freedom that move on different time scales. Under this assumption, we can reasonably expect that the $H_2$ fast motion will take place as if the other coordinate were frozen in one of its initial configurations. Nonetheless, using the PSA we can still model energy transfer to and from the surface degrees of freedom. *A priori*, $H_2$/Cu seems an ideal system for the PSA, due to the high mass mismatch between the molecule and the substrate atoms and the weak phonon-molecule coupling [56].

## 4. Results and discussion

### 4.1 Comparison between p3m1 and p6m potentials

The potential energy surface that we used in our calculations on the static surface differs from the one previously adopted in [16] in the symmetry of the surface. Since we had to distinguish the hcp sites – above the moving 2$^{nd}$ layer copper atom – from the fcc sites, we had to drop the approximation made in the earlier work [16] where the interaction with the fcc site equals that with the hcp site. Therefore, we lower the symmetry of the PES from p6m ($C_{6v}$ point group) to p3m1 ($C_{3v}$ point group) [25]. In the top panel of Fig. 4, we compare the static surface reaction probability obtained fixing the $Q$ coor-

**Table 2.** Properties of the transition states for the high symmetry sites.

| Site | Weight | ZPE (eV) | $Z_b$ (Å) | $r_b$ (Å) | $E_b$ (eV) |
|---|---|---|---|---|---|
| bridge | 3/12 | 0.173 | 1.16 | 1.02 | 0.618 |
| t2f | 3/12 | 0.197 | 1.26 | 1.26 | 0.768 |
| t2h | 3/12 | 0.198 | 1.26 | 1.26 | 0.779 |
| top | 1/12 | 0.208 | 1.38 | 1.40 | 0.880 |
| fcc | 1/12 | 0.181 | 1.25 | 1.47 | 0.995 |
| hcp | 1/12 | 0.188 | 1.25 | 1.51 | 1.009 |

dinate at the equilibrium position and the same result computed with the PES by Díaz *et al.*

The two dissociation probability curves have approximately the same reactive threshold, but the p3m1 PES is more reactive than the p6m PES at higher collision energies. A possible reason of this discrepancy can be found by analyzing the reaction probability when the $X, Y$ components of the $H_2$ center of mass are fixed at one of the high symmetry sites of the surface depicted in Fig. 2. This 4D reaction probability is plotted as a function of the incident energy in the lower panel of Fig. 4.

To investigate the contribution that each site makes to the global reactivity, we have applied two corrections to the probability curves: we have multiplied them by the relative weight of the site and we have translated them along $E_{\text{inc}}$ to take into account the difference in Zero Point Energy (ZPE) at the transition states (as in [8]). In Table 2, we report the properties of the transition states calculated by fixing the $(X, Y)$ coordinates of the center of mass of the hydrogen molecule at one of the high symmetry sites and the polar angle $\vartheta$ equal to 90° (molecule parallel to the surface).

From the results reported, we see that for $(v = 0, J = 0)$ and for collision energies lower than $\sim 0.7$ eV the reaction mainly takes place at the bridge site, for both the p3m1 and p6m PESs. On the other hand, at higher collision energies the t2h/t2f sites become important as well: they become as reactive as the bridge site and have the same relative weight over the total unit cell. Therefore, at high collision energies the p3m1 PES is more reactive than the p6m PES, because in the p3m1 PES the t2f and fcc barrier heights are lower than in the p6m PES. In the p6m PES these barrier heights are based on DFT calculations for the t2f and hcp geometries, so that they are larger.

### 4.2 Dissociative chemisorption

In Fig. 5, we report the results of lower dimensional quantum dynamics calculations, in which $X, Y$ have been fixed at one of the high symmetry sites of the surface, resulting in different 5D dynamical models. The reaction probability has been computed for the initial state $v = 0$, $J = 0$ of the $H_2$ molecule and different surface conditions: the static surface, the ground state $n = 0$, and the excited state $n = 6$ (where $n$ is the quantum number labelling the eigenstates of the phonon coordinate).

First of all, we can compare the static surface and the $n = 0$ results. We see that the introduction of the surface vibrational degree of freedom with its initial zero point energy has little or no effect. For the bridge site, for which the static surface curve show

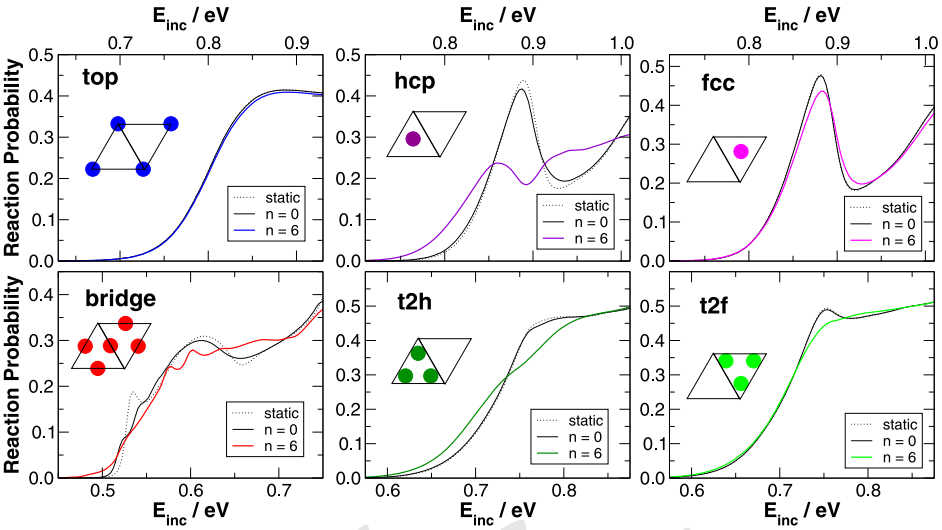


**Fig. 5.** 5D reaction probabilities for $H_2$ in the $v = 0$, $J = 0$ initial state and the $X, Y$ components of the $H_2$ center of mass fixed to a high symmetry site, as a function of the incident energy. Results are reported for the static surface (dotted line), the ground state $n = 0$ (solid black line) and the excited state $n = 6$ (solid colored line).

some structure due to resonances, the reaction probability is smoothened. This seems to indicate that in general surface lattice motion – even with the surface at 0 K – may indeed lead to the disappearence of structures due to quantum resonances in the state selected reaction probability. This problem has been debated in the past for reactive scattering of $H_2$ from Pd(100). Guided by the theoretical predictions of Gross *et al.* [23], Rettner and Auerbach looked for resonances in the reaction probability of $v = 0$, $J = 0$ $H_2$ without success [53,54]. The possibility that this could be an effect of phonons was discussed, but an estimate based on the surface mass model was not enough to explain the observation. Our result seems to indicate that not only the mechanical coupling to phonons, as introduced by the surface mass model, but also the electronic coupling acts in the direction of smoothening the fine structure of quantum mechanical reaction probabilities. When considering the coupling to all the lattice degrees of freedom, it is then likely that a complete removal of the resonance structure could be achieved.

By comparing the $n = 0$ and $n = 6$ results, we can consider the effect of vibrational excitation of the surface on the reaction probability. For impact on the bridge, t2h and hcp sites, the effect of surface vibrational excitation is to broaden and smoothen the reaction probability, with the effect being most dramatic over the hcp site itself. For the other sites the coupling is very small, and consequently the change of the reaction probability is also very small for vibrationally excited states of the surface.

We can now consider the results for the full dimensional 7D model in which also motion in $X, Y$ is directly included in the calculation. In Fig. 6, the reaction probability of $H_2$ in the $v = 0$, $J = 0$ state is reported for different surface descriptions: for a full 7D quantum calculation, with the surface initially in the $n = 0$ or $n = 9$ state ($Q$ 7D), for a PSA calculation, with the surface initially in the $n = 0$ or $n = 9$ state ($Q$ 6+1D),

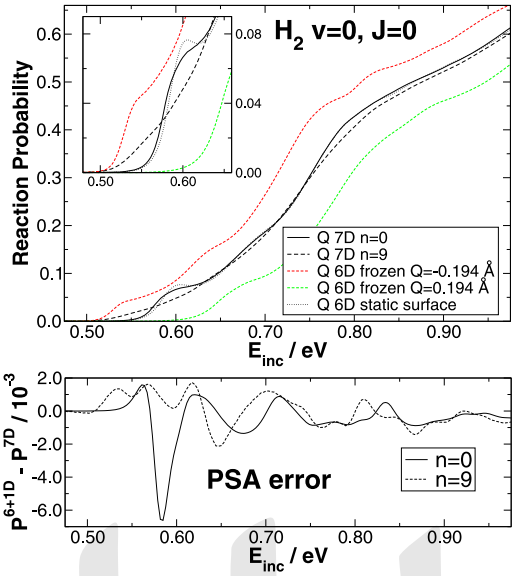


**Fig. 6.** 7D reaction probabilities of $H_2$ in the $v = 0$, $J = 0$ initial state as a function of incident energy. Top panel: in black lines, respectively solid and dashed, the $Q$ 7D results for $n = 0$ and $n = 9$; in dotted line, the $Q$ 6D static surface result; in colored dashed lines, the $Q$ 6D frozen results, in red for $-0.194$ Å and in green for $+0.194$ Å. Bottom panel: the error of the PSA, with the solid line for $n = 0$ and the dashed line for $n = 9$.

for a 6D quantum calculation, with $Q$ frozen at the equilibrium position ($Q$ 6D static surface) and for a 6D quantum calculation with $Q$ frozen at $-0.194$ Å, $+0.194$ Å ($Q$ 6D frozen).

As in the lower dimensional calculations, we can first consider the 6D static surface and the 7D $n = 0$ results. From this comparison, we see that introducing the additional degree of freedom and imparting zero point energy in it have little effect on the reaction probability. According to our model, the static surface approximation works very well for the vibrational ground state of the lattice atoms. On the other hand, comparing the $n = 0$ and $n = 9$ 7D results, we see that the effect of vibrational excitation of the lattice coordinate is to broaden and smoothen the reaction probabilities. In particular, there is a significant increase at lower incident energies where no reaction takes place in the static surface calculation.

The PSA appears to be an extremely good description of the lattice motion effects (see bottom panel of Fig. 6). The biggest difference occurs at energies where the reaction for $n = 0$ appears to be affected by a resonance, which may be hard to capture with the sudden approximation. Since the idea behind PSA is that the reaction probability is an average of reaction probabilities over the surface atom positions, it is interesting to examine what happens when $Q$ is frozen in displaced configurations. From the results plotted ($Q$ 6D, frozen in Fig. 6), it can be seen that the effect of the surface atom displacement is to shift the reaction probability to lower or higher incident energy. This is expected on the basis of the barrier height change discussed in relation to Fig. 1. The

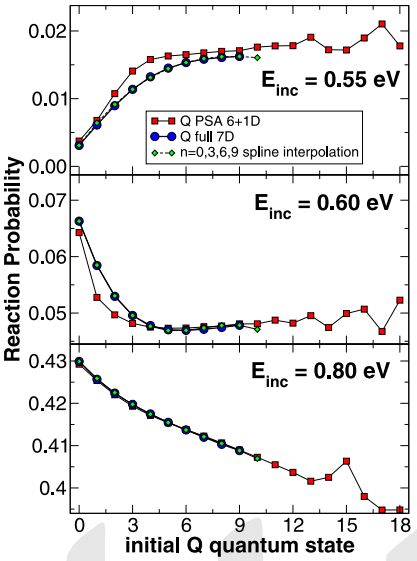


**Fig. 7.** 7D reaction probabilities of $H_2$ in the $v = 0$, $J = 0$ initial state as a function of $Q$ vibrational state, for three different incident energies (from top to bottom, $E_{inc} = 0.55$ eV, 0.60 eV, 0.80 eV). Full 7D results (blue circles), 6 + 1D sudden results (red squares) and interpolated 7D results based on calculations with $n = 0,3,6$ and 9 (green diamonds). Lines between the points are plotted to guide the eye.

**Table 3.** CPU times and memory required for thermally averaged results, with the three schemes: full 7D calculations performed on 10 initial states, sudden approximation 6 + 1D calculation with 20 quadrature points for $Q$ and 7D calculations for $n = 0, 3, 6, 9$ and spline interpolation for obtaining results for other $n$ values.

| Scheme | Time (h) | Memory (GB) |
|---|---|---|
| Full 7D, $n = 0$–9 | 23 744 | 392 |
| Sudden 6 + 1D | 4544 | 36 |
| Full 7D, $n = 0, 3, 6, 9$ | 9498 | 392 |

broadening hence is approximately the result of averaging reaction probabilities shifted at different incident energies.

In Fig. 7, reaction probabilities are reported for $v = 0$, $J = 0$ $H_2$ as a function of the $Q$ vibrational state for three different incident energies. Three methods are compared: the full 7D quantum wavepacket method ($Q$ full 7D), the 6 + 1D PSA method ($Q$ PSA 6 + 1D) and the full 7D using spline interpolation of results for $n = 0,3,6,9$ ($n = 0,3,6,9$ spline interpolation). The three incident energies were chosen in correspondence to the highest effect of vibrational excitation (see Fig. 6)

From the graph, we see that the reaction probability smoothly depends on the quantum number of the surface $n$. As a result, spline interpolation of the 7D results gives almost exact results, and as we will discuss later this can effectively be used to reduce the number of vibrational states to be considered to perform a thermal average (see Table 3).

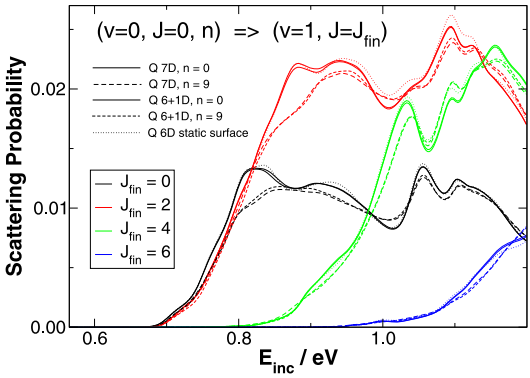


**Fig. 8.** Vibrationally inelastic scattering probabilities from the ($v = 0,\ J = 0$) state to the ($v = 1,\ J = 0, 2, 4, 8$) states as a function of incident energy of the $H_2$ molecule. Different colors mark different final rotational states. In thick lines, respectively solid and dashed, the $Q$ 7D results for $n = 0$ and $n = 9$. In thin lines, again solid and dashed, the $Q$ 6+1D results for $n = 0$ and $n = 9$. The dotted line is the $Q$ 6D static surface result.

As already shown in Fig. 6, the vibrational sudden approximation gives results in good agreement with the exact full quantum dynamical calculations. The error is higher at low incidence energy, near the reaction threshold, where the PSA seems to overestimate the effect of $Q$ excitation, which, as already noted, may be due to a resonance effect. Furthermore, it should be noted that for $n$ greater than 12–13, some oscillations appears in the reaction probability. However these are most likely due to the quadrature error in the sudden average, rather than to the PSA itself.

### 4.3 Vibrationally inelastic scattering

We now analyze the effect of lattice motion on the vibrationally inelastic scattering from the ($v = 0,\ J = 0$) state to the ($v = 1,\ J = 0, 2, 4, 6$) states. In Fig. 8, results are reported as a function of the incidence energy of the hydrogen molecule. The surface descriptions defined above in the case of dissociative chemisorption are used also in this case.

Regardless of the surface description, our calculations predict the inelastic scattering to have the same threshold for both the ($v = 1,\ J = 0$) and ($v = 1,\ J = 2$) states, but with the latter having higher probability. On the other hand, the inelastic scattering probability to $J = 4$ and $J = 6$ are shifted to increasingly higher incident energy.

Concerning the effect of surface vibration, the results are in line with the ones obtained for the dissociative process. The effect of the inclusion of the degree of freedom in its ground state is almost negligible. This again supports the use of a static surface approximation in the case of low temperature surface. The vibrational excitation of the surface degree of freedom (in this case to $n = 9$), on the other hand, gives a slight decrease of the scattering probabilities. This effect is well captured by the PSA, which predicts scattering probabilities in excellent agreement with full quantum dynamics.

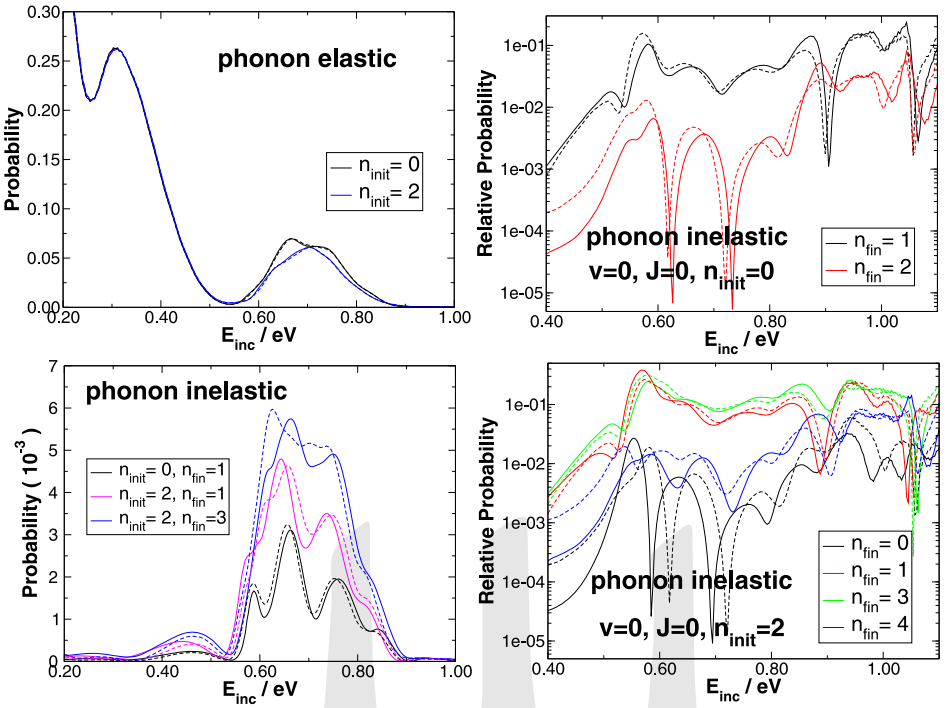


**Fig. 9.** Rovibrationally and diffractionally elastic scattering as a function of the $H_2$ incident energy, for the molecule in the initial $v = 0$, $J = 0$ state and the surface phonon in the $n = 0{,}2$ states. In the top left panel, the elastic scattering probabilities. In the lower left panel, the phonon inelastic scattering probabilities for the transitions with $\Delta n = \pm 1$. In the two right panels, phonon inelastic scattering probabilities are reported on a logarithmic scale and normalized to the elastic scattering probability, according to the ratio: $P(v, J, n \to v, J, n')/P(v, J, n \to v, J, n)$. All results are plotted both for the full 7D $QD$ (solid lines) and the $6+1$D PSA calculation (dashed lines).

## 4.4 Phonon elastic and inelastic scattering

In Fig. 9, we report the probability of rovibrationally and diffractionally elastic scattering, *i. e.* the probability that the molecule is scattered with the same rovibrational state and the same parallel momentum, with the surface either in the same vibrational state ("phonon-elastic" scattering) or in a different state ("phonon-inelastic" scattering). In the graph we have plotted the results for two different initial conditions for the surface degree of freedom, namely the $n = 0$ and $n = 2$ states, and we have only included those final states for which we found a non negligible probability.

The results we obtained show that the phonon-elastic probability of this event is strongly attenuated by the increase of incident energy, up to 1.0 eV at which we have almost no probability. This is mostly due to the competition with the channels already included in the 6D model, in which $H_2$ can undergo rovibrationally inelastic transitions, diffraction or dissociation. However the results suggest that also the substrate plays a relevant role: in the range of collision energy between 0.50 eV and 0.90 eV, there is

a clear difference between the probability for the $n = 0$ and the $n = 2$ vibrational states of the surface, with the latter giving less phonon elastic scattering.

This is confirmed by considering the phonon inelastic scattering, the scattering event in which only the surface state is changed, hence involving an actual transfer of the incident kinetic energy from the molecule to the surface and *vice versa*. On a general note, we see that the magnitude of the probability depends on the number of quanta required by the transition. Probabilities for transitions involving more than two quanta are negligible. In the incident energy interval 0.50–0.90 eV, the probabilities of the transition involving a single quantum (from $n = 0$ to $n = 1$ and from $n = 2$ to $n = 1, 3$) become of the order of one tenth of the elastic scattering probability, and hence become relevant for the overall outcome of the scattering process. These results suggest that phonon inelastic scattering probabilities will be larger for initial states with $n > 0$, because in this case two transitions with $\Delta n = 1$ are possible. Also, the probability for $\Delta n = +1$ appears to be larger for the $n = 2$ state than for the $n = 0$ state. This results in a different exchange of energy with the molecule for $n > 0$.

Finally, extrapolating the results to the lower energies relevant for the experiments on $H_2$ diffraction [20] suggests that energy transfer to second layer copper atoms should have little effect on specular scattering of $H_2$ from Cu(111) at energies of experimental interest.

We have computed all the phonon elastic and inelastic probabilities with both exact and PSA dynamics. The calculation of the phonon inelastic scattering probability can be considered as the most demanding test on the Phonon Sudden Approximation that we can perform. Since in the $6 + 1$D results the dynamical coupling between $H_2$ and the surface has been approximated, we could expect the energy transfer to be the quantity that is most severely affected. However, from the results we see reasonable agreement between exact and PSA dynamics. In detail, we see that the behaviour of the curves is very well reproduced by the PSA. There are significant quantitative differences, but on an absolute scale the phonon inelastic probabilities themselves are very low in any case.

### 4.5 Thermal averages

We can now turn our attention to the thermal averages of the observables described so far. This allows us to consider how our description of the surface could affect the results in the realistic experimental situation of scattering from a surface at some finite $T_S$.

Three different strategies to compute the thermal averages were used. As benchmark, we computed the Boltzmann average of the probabilities corresponding to the entire range of $Q$ vibrational states up to $n = 9$ (the convergence of this results with respect to the maximum $n$ value was tested for $T_S = 925$ K). Starting from the sudden approximation results it was possible to directly compute the thermal average from the lower dimensional 6D calculations. However, a proper quadrature scheme along $Q$ has to be defined. In our case we tested and then adopted a Gauss-Hermite quadrature with 20 grid points. Finally, in some cases we exploited the smoothness of the reaction probability as a function of the vibrational state $n$ (cf. Fig. 7): we computed only the reaction probability for the initial states $n = 0, 3, 6, 9$, we interpolated for other values and then evaluated the thermal average.

Table 3 reports the time and memory that we used to compute the reaction probability for $H_2$ in $v = 0$, $J = 0$ as a function of the temperature of the surface, with these

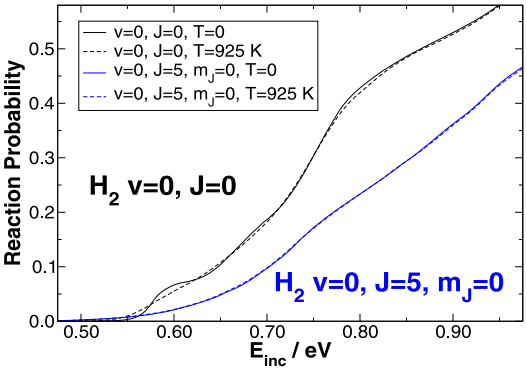


**Fig. 10.** 7D reaction probabilities of $H_2$ as a function of incident energy for different surface temperature, $T = 0$ K (solid lines) and $T = 925$ K (dashed lines). In black results for the initial ($v = 0$, $J = 0$) state, and in blue results for the initial ($v = 0$, $J = 5$, $M_J = 0$) state are presented.

three strategies. The data reported refers to a clustered system of IBM Power6+ 32 core nodes using Infiniband. Each type of calculation was performed with the most convenient parallelization scheme that was doable in that case. The PSA calculations had lower memory requirements and we could use the less expensive OPENMP parallelization. On the other hand, 7D calculations required more than one node and consequently we had to use MPI communication (MPI version 2.1). As can be seen, with both the PSA and the spline interpolation we could achieve a large reduction of the calculation time. On the other hand, the PSA is the only way to also reduce the memory requirement. Finally, the PSA calculations offer excellent opportunities for parallelization, as the 6D calculations for each value of $Q$ can be run simultaneously on separate nodes (or sets of nodes) with little communication between the nodes (or sets of nodes) required.

In addition to computational performance, we also checked the accuracy of the PSA for thermally averaged results. Comparing $6+1$D and 7D probabilities both for reactive and vibrationally inelastic scattering (not reported here), we found that there is an even better agreement for the thermal averaged results. This can be reasonably expected, since the sudden approximation works better for lower $n$ states and these states have the largest weights in the thermal average.

Figure 10 shows the thermal average of the reaction probability of $H_2$ in the ($v = 0$, $J = 0$) and ($v = 0$, $J = 5$, $M_J = 0$) initial states, as a function of the incident energy. The mean values have been computed assuming a Boltzmann distribution and including the states up to $n = 9$. We have checked the convergence of this average with respect to the number of vibrational states, and found that 10 states (that represent more than 90% of probability) are enough to get accurate results (data not shown). We considered the temperatures $T_S = 0$ K and $T_S = 925$ K, with the latter being the temperature in the associative desorption experiments by Rettner and Auerbach [50].

The average for the state ($v = 0$, $J = 0$) has been computed from all the ten 7D calculations with $n$ ranging from 0 to 9. On the other hand, for ($v = 0$, $J = 5$, $M_J = 0$) only the reaction probability for the states $n = 0, 3, 6, 9$ has been directly obtained from wavepacket dynamics. The probability for the other $n$ values has been found by interpo-

lation with a cubic spline function of n, with the scheme already discussed in relation to Fig. 7. In the incidence energy range we are interested in, this approximation is very good and does not affect the accuracy of the thermal average at all.

We immediately note that the effect of surface temperature predicted by our model seems to be extremely small, clearly less than suggested by experiments [37,40] and by predictions of other theoretical models [41,62]. There are at least three problems that should be considered, that can explain the inadequacy of our model in reproducing the experimental results.

Firstly, it has been shown in other theoretical works that lattice expansion may play a role in affecting the reaction probability. From DFT calculations, it was found by Nattino *et al.* that the lowest barrier to reaction is reduced by 35 meV at $T_S = 925$ K due to lattice expansion effects [41]. This is consistent with the d-band model of $H_2$/metal interaction: as described in [57], the expansion of the lattice leads to a higher hydrogen reactivity due to a smaller overlap between the metal orbitals. From a dynamical point of view, the lattice expansion hence may be reflected in a shift of the reaction probability to lower incident energy.

Secondly, other surface degrees of freedom could be important. From the analysis of the energetic coupling, we pointed out in previous work that at least the motion of a first layer atom should be considered, both in the parallel and perpendicular direction. Furthermore, we cannot fully exclude the importance of non-additive couplings between the lattice degrees of freedom, even if they seem to be on a smaller energy scale [3] and even if the work by Wijzenbroek *et al.* showed that a qualitatively consistent model for surface temperature can be built by simply considering uncoupled lattice atoms [62].

Finally, apart from the neglect of the other important effects, also within the present model we could obtain a greater effect with the same magnitude of the coupling but with different oscillator frequency, as was first pointed out by Dohle and Saalfrank in relation to their model approaches to lattice motion [19]. The surface coordinate that we have chosen is localized and highly coupled to other lattice coordinates, but we considered it as if it was completely uncoupled. Within a full description of the Cu slab, there are true phonons including a perpendicular displacement of the second layer atoms with a lower harmonic frequency than the one adopted in the present work. This can act in two directions. On the one hand, this leads to vibrational eigenstates that have higher probability far from the equilibrium position. On the other hand, the associated Boltzmann distribution has a higher population of the excited states. These two effects act in the same direction: they give a higher probability to find the vibrational coordinate far from the equilibrium position, and can effectively increase the broadening. Figure 11 illustrates this point: we lowered the frequency of $Q$ in the PSA average from $\omega = 19$ meV, the proper value for our 7D potential, to $\omega = 13.5$ meV, the frequency of a true phonon that includes perpendicular displacement of a 2$^{nd}$ layer copper atom. The effect on the reaction probability is more than doubled, especially at higher incident energies.

We now consider the experiment on vibrational inelastic scattering performed by Rettner *et al.* [51], who measured the Time of Flight (TOF) of molecules scattered from all ($v = 0$, $J$) states to the ($v = 1$, $J = 3$) state, with the surface at $T_S = 400$ K, 700 K. Previous simulations of the TOF spectrum with Born-Oppenheimer static surface quan-

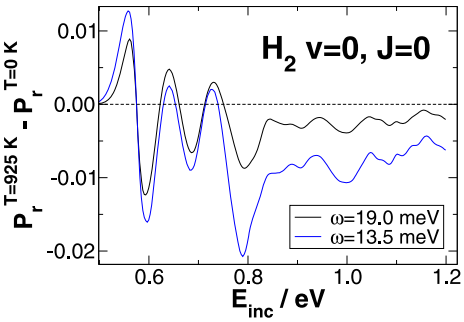


**Fig. 11.** Difference between reaction probabilities at $T = 0$ K and $T = 925$ K, computed with different frequencies of the $Q$ oscillator within the PSA: in black $\omega = 19$ meV, the frequency of the 7D potential employed in the present work and in blue $\omega = 13.5$ meV, the lowest frequency of a phonon including the perpendicular displacement of a 2nd layer atom, in the phonon spectrum of our Cu supercell.

tum dynamics underestimated the vibrational excitation probability by a factor of 3 [18]. In [34] it is suggested that this discrepancy could be reduced by taking into account the thermal motion of the surface. In fact, the intensity of the TOF signal reflects not only the probability of scattering to the ($v = 1$, $J = 3$) state, but also the energy loss to the surface (including loss to surface phonons), since molecules which have lost part of their incidence energy travel more slowly in the detection zone and thereby increase the detection signal [34,51].

Díaz *et al.* showed that the most important contribution to the ($v = 1$, $J = 3$) TOF signal comes from the ($v = 0$, $J = 5$) initial state [16]. As vibrational excitation from one (v, J) state to all states with $v' = v + 1$ is also of interest, we will consider two processes: the scattering from ($v = 0$, $J = 0$) to all $v = 1$ states and from ($v = 0$, $J = 5$, $M_J = 0$) to all $v = 1$ states. We chose $M_J = 0$ because this angular momentum projection gives the highest vibrationally inelastic scattering probability.

In Fig. 12, the thermal average of the total scattering probability to $v = 1$ is shown, for the ($v = 0$, $J = 0$) and ($v = 0$, $J = 5$, $M_J = 0$) initial states of $H_2$ and varying the surface temperature. To compute the thermal average, we have followed the same methodology described before for the reaction probability. We have considered the surface temperature $T_S = 700$ K, the highest $T_S$ reported in the experiments [51].

As in the case of the reaction probability, the effect of $Q$ thermal excitation on the probability is very small. Furthermore, it does not go in the direction which we expect from the experimental results, since the inclusion of the new degree of freedom slightly lowers the scattering probability. Even the effect of the frozen displacement $Q = -0.194$ Å, $+0.194$ Å is very small. The results hence suggest that the effect of the 2nd layer atom cannot in any way be responsible for an increase in vibrationally inelastic scattering probability.

This can indeed be explained from what is known theoretically about this process. Calculations showed that efficient vibrational excitation can occur if the system shows a late barrier and a reaction path with a large curvature in front of the barrier. In the case of Cu(111), these conditions are satisfied near the top site [33]. The coupling to the vibration of the 2nd layer atom is particularly small for the top site, as can be seen

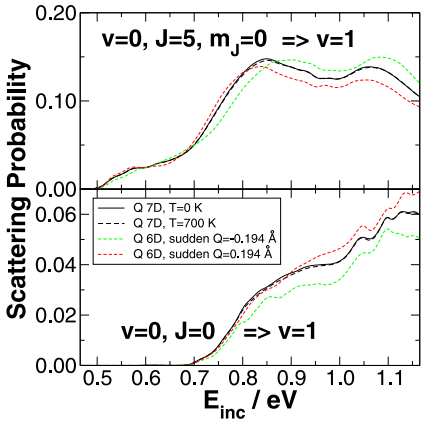


**Fig. 12.** 7D vibrationally inelastic scattering probabilities of ($v = 0$, $J = 0$) $H_2$ (top panel) and ($v = 0$, $J = 5$, $M_J = 0$) $H_2$ (lower panel) to the $v = 1$ states as a function of incident energy, for the surface temperatures $T_S = 0$ (black solid line) and $T_S = 700$ K (black dashed lines). In addition, the 6D scattering probabilities for two frozen displacements, $Q = -0.194$ Å, $+0.194$ Å, are shown using red and green dashed lines, respectively.

in Fig. 1. For this reason we expect that the motion of the 1st layer atoms may affect the vibrationally inelastic scattering probability more than the 2nd layer.

Furthermore, as we mentioned the fraction of translational energy transfered from the molecule to the surface is a critical quantity for the description of the vibrationally inelastic scattering experiments. In the case of scattering of ($v = 0$, $J = 0$) $H_2$, our results predict that the vibrationally excited molecules have transfered less than 3 meV to the surface, in the range of $E_{inc}$ considered (0.6–1.2 eV). This amount of energy is far below what can be reasonably expected for this kind of experiment, which is around 30% of the incidence energy [34]. This analysis indicates that other surface degrees of freedom with a more efficient energy transfer should be considered to achieve a better description of the vibrationally inelastic scattering experiments [51] than obtained so far [34].

## 5. Conclusions

In this work we have developed and studied a 7D quantum dynamical model for scattering of $H_2$/Cu(111). This model includes a single surface coordinate, representing the perpendicular motion of a second layer lattice atom. This degree of freedom mostly induces electronic effects in the dissociative reaction path, *i. e.* it can modulate the height of the barrier to dissociation without changing the geometrical properties of the PES much.

With this model, we have investigated surface motion effects for different observables: the reaction probability, the vibrational excitation probability and phonon-state selected probabilities. In addition, these properties were employed to extensively test the validity of the vibrational sudden approximation, applied to the surface phonon.

The first indication that we get from our results is that the static surface approximation is a very good description of the surface at low temperature. At $T_S = 0$ K, the probability distribution of the copper atom around the equilibrium position is not broad and the higher or lower reactivity coming from configurations with lower or higher barrier compensate each other.

Furthermore, our model gives indications on how the vibrational excitation of an electronically coupled lattice coordinate affects the dynamical processes. First of all, the lattice excitation averages out structures such as quantum resonances that might be present in the static surface model, resulting in curves that are smoother as a function of incident energy. In the case of dissociative adsorption, we observed a small broadening of the reaction probability with an increase of the probability at lower incident energy where almost no reaction takes place with the static surface. On the contrary, the $H_2$ vibrational excitation probability as a function of incident energy is a bit decreased with respect to the static surface results. Finally, the rovibrationally and diffractionally elastic scattering of $H_2$ is changed by the competition with phonon inelastic scattering channels, which appears to have a relevant effect in the incident energy interval 0.50–0.90 eV.

We also computed thermal averages to study the dependence of the observables considered on the surface temperate. However, we found that our model seems to be insufficient for the description of the experimental observations. In the case of associative chemisorption of $H_2$, the broadening effects are consistent with experiments, but on a much smaller scale. In the case of $H_2$ vibrational excitation, there is also a qualitative discrepancy. Hence, it seems that for a comparison with experiments other effects should be included as well, like lattice expansion and first layer lattice motion.

All the surface vibrational excitation effects we observed are extremely well reproduced within the Phonon Sudden Approximation picture of lattice motion. The PSA allowed us to describe all the relevant scattering and reactive processes with high accuracy. We even obtained a reasonable description of the energy transfer to the surface, the most challenging test for an approximation on the molecule-surface coupling itself.

In conclusion, our investigation shows two important results: (i) the effect of the perpendicular motion of the second layer surface atom can be accurately described with a sudden approximation, which neglects dynamic coupling between molecular motion and this particular surface motion (*i. e.*, "recoil effects") but still includes *quasi*-static effects, and (ii) surface temperature effects of this particular surface motion we investigated are small, and cannot account for the main experimental findings, even with full 7D dynamics. This suggests that our model is incomplete, and that we should also take into account the effects of motion of first layer surface atoms, and possibly also effects of surface expansion.

The PSA approach appears to be extremely promising for the $H_2 + Cu(111)$ system. In future, we plan to consider the inclusion of an $8^{th}$ degree of freedom, the motion of the nearest first layer atom perpendicular to the surface, to achieve a dynamical model that describes the most important lattice motions in the direction perpendicular to the surface. Furthermore, an even larger dynamical model with the full three dimensional motion of a first layer atom nearest to $H_2$ could also be doable. For each additional degree of freedom, 7D and $6+1$D quantum dynamical calculations can be used to assess whether (i) the additional degree of freedom is relevant for the

description of surface temperature effects, (ii) the sudden approximation is good at modeling these effects. These studies can guide us in the development of efficient high dimensional models including the degrees of freedom that are most relevant for describing surface temperature effects, using a sudden approach for specific surface degrees of freedom if this approximation appears to be appropriate. In this development, we will take into account that for a PSA calculation including more than two sudden degrees of freedom, a standard quadrature over the phonon coordinates could be too expensive. However, a Monte Carlo approach could still be used to sample the configurations of the copper atoms and to compute the difference between the static surface and thermal probabilities, within the framework of a quantum dynamical method using the PSA. In fact, such a way of sampling the phonon coordinates has already effectively been used in quasi-classical dynamics calculations sampling the coordinates of several surface atoms in what may be called a classical sudden approach [62].

In conclusion, in future we plan to include the surface atom motions in the dynamical model using a potential energy surface with just few additional degrees of freedom (three for the first layer and one for the second layer). For such a study to be feasible, a quantum dynamics approach that scales favourably with the system dimension is required. In the present work we have shown that the Phonon Sudden Approximation gives very accurate results at a low computational cost, and hence appears to be an excellent choice for the purpose of studying the most important *quasi*-static effects of the surface motion on the relevant scattering events.

## Acknowledgement

This work was supported by a TOP grant from NWO/CW and by a grant of computer time from NCF. We thank SURFsara (www.surfsara.nl) for the support in using the Dutch national super computer Huygens. C. Díaz acknowledges support under MICINN project FIS2010-15127. We also thank Mark Wijzenbroek for useful discussions.

## References

1. S. R. Bahn and K. W. Jacobsen, Comput. Sci. Eng. **4** (2002) 56.
2. H. F. Berger, M. Leisch, A. Winkler, and K. D. Rendulic, Chem. Phys. Lett. **175** (1990) 425.
3. M. Bonfanti, C. Díaz, M. F. Somers, and G.-J. Kroes, Phys. Chem. Chem. Phys. **13** (2011) 4552.
4. J. M. Bowman, G. Drolshagen, and J. P. Toennies, J. Chem. Phys. **71** (1979) 2270.
5. H. F. Busnengo, A. Salin, and W. Dong, J. Chem. Phys. **112** (2000) 7641.
6. Y.-Y. Chuang, M. L. Radhakrishnan, P. L. Fast, C. J. Cramer, and D. G. Truhlar, J. Phys. Chem. A **103** (1999) 4893.
7. J. Dai and J. C. Light, J. Chem. Phys. **107** (1997) 1676.
8. J. Dai and J. C. Light, J. Chem. Phys. **107** (1997) 1676.
9. J. Dai and J. C. Light, J. Chem. Phys. **108** (1998) 7816.
10. J. Dai, J. Sheng, and J. Z. H. Zhang, J. Chem. Phys. **101** (1994) 1555.
11. J. Dai and J. Z. H. Zhang, Surf. Sci. **319** (1994) 193.
12. J. Dai and J. Z. H. Zhang, J. Chem. Phys. **102** (1995) 6280.
13. G. R. Darling and S. Holloway, J. Chem. Phys. **97** (1992) 734.

14. G. R. Darling and S. Holloway, Surf. Sci., **307** (1994) 153.
15. G. R. Darling and S. Holloway, J. Chem. Phys. **101** (1994) 3268.
16. C. Díaz, R. A. Olsen, D. J. Auerbach, and G.-J. Kroes, Phys. Chem. Chem. Phys. **12** (2010) 6499.
17. C. Díaz, R. A. Olsen, H. F. Busnengo, and G.-J. Kroes, J. Phys. Chem. C **114** (2010) 11192.
18. C. Díaz, E. Pijper, R. A. Olsen, H. F. Busnengo, D. J. Auerbach, and G.-J. Kroes, Science **326** (2009) 832.
19. M. Dohle and P. Saalfrank, Surf. Sci. **373** (1997) 95.
20. D. Farías and R. Miranda, Prog. Surf. Sci. **86** (2011) 222.
21. B. Gergen, H. Nienhaus, W. H. Weinberg, and E. W. McFarland, Science **294** (2001) 2521.
22. A. Groß, B. Hammer, M. Scheffler, and W. Brenig, Phys. Rev. Lett. **73** (1994) 3121.
23. A. Gross, S. Wilke, and M. Scheffler, Phys. Rev. Lett. **75** (1995) 2718.
24. S. J. Gulding, A. M. Wodtke, H. Hou, C. T. Rettner, H. A. Michelsen, and D. J. Auerbach, J. Chem. Phys. **105** (1996) 9702.
25. T. Hahn (ed.), *International Tables for Crystallography*, vol. A (Space-Group Symmetry), 5th edition, Wiley, Hoboken, 2005.
26. B. Hammer and J. K. Nørskov, Surf. Sci. **343** (1995) 211.
27. B. Hammer, L. B. Hansen, and J. K. Nørskov, Phys. Rev. B **59** (1999) 7413.
28. B. Hammer, M. Scheffler, K. W. Jacobsen, and J. K. Nørskov, Phys. Rev. Lett. **73** (1994) 1400.
29. M. Hand and J. Harris, J. Chem. Phys. **92** (1990) 7610.
30. A. Hodgson, J. Moryl, P. Traversaro, and H. Zhao, Nature **356** (1992) 501.
31. A. Hodgson, P. Samson, A. Wight, and C. Cottrell, Phys. Rev. Lett. **78** (1997) 963.
32. H. Hou, S. J. Gulding, C. T. Rettner, A. M. Wodtke, and D. J. Auerbach, Science **277** (1997) 80.
33. G.-J. Kroes, Prog. Surf. Sci. **60** (1999) 1.
34. G.-J. Kroes, C. Díaz, E. Pijper, R. A. Olsen, and D. J. Auerbach, Proc. Natl. Acad. Sci. USA **107** (2010) 20881.
35. J. E. Lennard-Jones, Trans. Faraday Soc. **28** (1932) 333.
36. L. Martin-Gondre, M. Alducin, G. A. Bocan, R. Díez Muiño, and J. I. Juaristi, Phys. Rev. Lett. **108** (2012) 096101.
37. H. A. Michelsen and D. J. Auerbach, J. Chem. Phys. **94** (1991) 7502.
38. H. A. Michelsen, C. T. Rettner, D. J. Auerbach, and R. N. Zare, J. Chem. Phys. **98** (1993) 8294.
39. R. C. Mowrey and G. J. Kroes, J. Chem. Phys. **103** (1995) 1216.
40. M. J. Murphy and A. Hodgson, J. Chem. Phys. **108** (1998) 4199.
41. F. Nattino, C. Díaz, B. Jackson, and G.-J. Kroes, Phys. Rev. Lett. **108** (2012) 236104.
42. S. Nave and B. Jackson, Phys. Rev. Lett. **98** (2007) 173003.
43. S. Nave and B. Jackson, J. Chem. Phys. **130** (2009) 054701.
44. S. Nave, D. Lemoine, M. F. Somers, S. M. Kingma, and G.-J. Kroes, J. Chem. Phys. **122** (2005) 214709.
45. R. A. Olsen, G.-J. Kroes, O. M. Løvvik, and E. J. Baerends, J. Chem. Phys. **107** (1997) 10652.
46. J. P. Perdew, J. A. Chevary, S. H. Vosko, K. A. Jackson, M. R. Pederson, D. J. Singh, and C. Fiolhais, Phys. Rev. B **46** (1992) 6671.
47. M. Persson, J. Strömquist, L. Bengtsson, B. Jackson, D. V. Shalashilin, and B. Hammer, J. Chem. Phys. **110** (1999) 2240.
48. E. Pijper, G. J. Kroes, R. A. Olsen, and E. J. Baerends, J. Chem. Phys. **117** (2002) 5885.
49. M. Polanyi and H. Eyring, Z. Phys. Chem. B **12** (1931) 279.
50. C. T. Rettner, D. J. Auerbach, and H. A. Michelsen, Phys. Rev. Lett. **68** (1992) 1164.
51. C. T. Rettner, H. A. Michelsen, and D. J. Auerbach, Chem. Phys. **175** (1993) 157.
52. C. T. Rettner, H. A. Michelsen, and D. J. Auerbach, J. Chem. Phys. **102** (1995) 4625.
53. C. T. Rettner and D. J. Auerbach, Phys. Rev. Lett. **77** (1996) 404.
54. C. T. Rettner and D. J. Auerbach, Chem. Phys. Lett. **253** (1996) 236.
55. T. Sahoo, S. Mukherjee, and S. Adhikari, J. Chem. Phys. **136** (2012) 084306.
56. T. Sahoo, S. Sardar, and S. Adhikari, Phys. Chem. Chem. Phys. **13** (2011) 10100.
57. S. Sakong and A. Groß, Surf. Sci. **525** (2003) 107.
58. J. Sheng and J. Z. H. Zhang, J. Chem. Phys. **99** (1993) 1373.

59. M. F. Somers, S. M. Kingma, E. Pijper, G.-J. Kroes, and D. Lemoine, Chem. Phys. Lett. **360** (2002) 390.
60. A. K. Tiwari, S. Nave, and B. Jackson, J. Chem. Phys. **132** (2010) 134702.
61. J. D. White, J. Chen, D. Matsiev, D. J. Auerbach, and A. M. Wodtke, Nature **433** (2005) 503.
62. M. Wijzenbroek and M. F. Somers, J. Chem. Phys. **137** (2012) 054703.